Polymer 49 (2008) 3950–3956

Contents lists available at ScienceDirect

Polymer

journal homepage: www.elsevier.com/locate/polymer

Magnetite nanoparticles stabilized with polymeric bilayer of poly(ethylene glycol) methyl ether–poly(ε-caprolactone) copolymers

Siraprapa Meerod [a], Gamolwan Tumcharern [b], Uthai Wichai [a], Metha Rutnakornpituk [a,*]

[a] Department of Chemistry, Faculty of Science, Naresuan University, Phitsanulok 65000, Thailand
[b] National Nanotechnology Center, National Science and Technology Development Agency, Pathumthani 12120, Thailand

ARTICLE INFO

Article history:
Received 25 April 2008
Received in revised form 2 July 2008
Accepted 3 July 2008
Available online 11 July 2008

Keywords:
Water dispersible
Magnetite
Nanoparticle

ABSTRACT

In this work, we report a synthetic method of water dispersible magnetite nanoparticles having oleic acid and poly(ethylene glycol) methyl ether–poly(ε-caprolactone) (mPEG–PCL) amphiphilic block copolymer as polymeric stabilizers. The particles were prepared by coprecipitation of Fe(II) and Fe(III) in NH_4OH and had bilayer surface with hydrophobic inner layer and hydrophilic corona. mPEG–PCL copolymer was synthesized by a ring-opening polymerization of ε-caprolactone using mPEG as a macroinitiator in the presence of stannous octoate catalyst. FTIR and thermogravimetric analysis (TGA) indicated the presence of the copolymer on the particle surface. Roles of reaction parameters, such as stabilizer concentrations and time of ultrasonicating treatment, on percent of magnetite in the complex and its magnetic properties were investigated. Transmission electron microscopy (TEM) showed the average particle size about 9.0 ± 1.1 nm in diameter. Vibrating sample magnetometry (VSM) measurement indicated that the magnetite nanoparticles were superparamagnetic at room temperature. Approximately $6.8 \pm 0.5\%$ of indomethacin model drug (68 μg/mg of magnetite) was effectively entrapped on the particles.

1. Introduction

Magnetite nanoparticles (Fe_3O_4) have long been of scientific and technological interests due to their unique physical and chemical properties [1–3]. Several potential applications of magnetite in bionanotechnology have been recently reported such as magnetic resonance imaging (MRI) enhancing agents [4–8], targeted drug delivery [9,10], hyperthermia treatment of tumors [11] and biomolecular magnetic separation and diagnosis [12]. The particles are usually stabilized by charge repulsion of electrical double layers [13] or steric repulsion of long-chain polymeric surfactants adsorbed on their surfaces to prevent approaching from neighboring particles [14]. Oleic acid has been markedly used as a steric stabilizer to form magnetite nanoparticles dispersed in organic solvents [15–17]. The stabilizing mechanism of the particles was proposed that carboxylate groups partitioned on the particle surface and formed a brush layer of long-chain hydrocarbon to sterically stabilize the particles in dispersions [18,19]. However, the oleic acid-coated magnetite particles were not dispersible in water and this limited their potential uses in biomedical applications. Many attempts have been made to prepare water dispersible magnetite particles by coating their surface with hydrophilic polymeric stabilizers [20–23]. In addition, surface modification of water dispersible particles to gain diverse and desirable properties has recently gained much attention. For instance, the particle surface can be coupled with functional molecules such as folic acid [24–31] or biological molecules such as DNA and antibodies [32,33].

Recently, several works have been focused on preparing water dispersible magnetite nanoparticles coated with polymeric bilayer and understanding the role of the polymers on colloidal stability [34,35]. Hatton et al. reported the synthesis of surfactant bilayer-stabilized magnetite nanoparticles using fatty acids as both primary and secondary surfactants to produce stable aqueous magnetic fluids [1]. A bipolar molecule such as tetramethyl-ammonium-11-aminoundecanoate was also used as the secondary surfactant in the oleic acid-coated magnetite to obtain water dispersible nanoparticles with narrow particle size distribution [36]. Jain et al. developed water-dispersible magnetite nanoparticles stabilized with bilayer surfactant of oleic acid/pluronic (poly(ethylene oxide)–poly(propylene oxide) copolymer) and studied their loading efficiency and releasing behavior of anticancer agents [37]. They proposed that poly(propylene oxide) blocks were physically adsorbed onto the particle surface coated with oleic acid primary surfactant, and poly(ethylene oxide) blocks provided steric stabilization. Riffle et al. reported the synthesis of triblock copolymers of polyurethane central blocks containing pendant carboxylate groups and polyether tail blocks such as poly(ethylene oxide). Magnetite nanoparticles were thought to complex with carboxylate groups and

* Corresponding author. Tel.: +66 5526 1000x3464; fax: +66 5526 1025.
E-mail address: methar@nu.ac.th (M. Rutnakornpituk).

0032-3861/$ – see front matter © 2008 Elsevier Ltd. All rights reserved.
doi:10.1016/j.polymer.2008.07.003

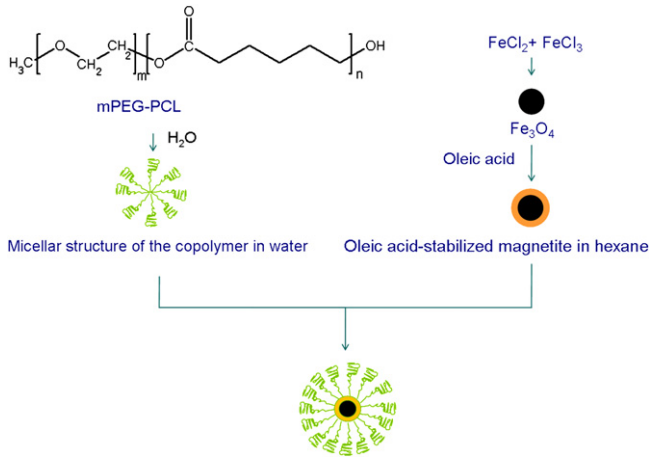

Fig. 1. Synthetic route of water dispersible magnetite nanoparticles stabilized with polymeric bilayer of oleic acid and mPEG–PCL amphiphilic block copolymer.

polyethers tail blocks extended to water and provided steric stabilization [38,39].

The primary aim of the current report is to prepare water dispersible magnetite nanoparticles containing hydrophobic inner shells for efficient entrapment of indomethacin model drug and hydrophilic outer layers for their good dispersibility in aqueous fluids (Fig. 1). Oleic acid in combination with amphiphilic block copolymers of poly(ethylene glycol) methyl ether (mPEG)–poly(ε-caprolactone) (PCL) were used as steric stabilizers for this purpose. Hydrophobic PCL blocks can hypothetically adsorb onto the pre-synthesized magnetite nanoparticles coated with oleic acid primary surfactant, and hydrophilic mPEG blocks can protrude outward from the particle surface to provide steric stabilization. mPEG–PCL copolymers were prepared *via* a ring-opening polymerization of ε-caprolactone using single hydroxyl-terminated mPEG as a macroinitiator in the presence of stannous octoate catalyst. The existence of the copolymers on the particle surface was evidenced by FTIR and thermogravimetric analysis (TGA) techniques. Particle size and its distribution were characterized using transmission electron microscopy (TEM). Vibrating sample magnetometry (VSM) measurement was carried out to study its magnetic properties at room temperature. Indomethacin-entrapped efficiency of the as-synthesized magnetite nanoparticles was also investigated.

2. Experimental section

2.1. Materials

Unless stated otherwise, all reagents and solvents were used without further purification. Poly(ethylene glycol) monomethyl ether (mPEG) with $\overline{M}_n$ 5000 g/mol (Acros) was dried in a vacuum oven at 60 °C under phosphorus pentoxide for 48 h. ε-Caprolactone (ε-CL) (99%, Acros) was stirred over CaH_2 at room temperature overnight and distilled prior to use. Stannous octoate (95%, Sigma), iron(III) chloride anhydrous ($FeCl_3$) (Carlo Erba), iron(II) chloride tetrahydrate ($FeCl_2{\cdot}4H_2O$) (Carlo Erba), ammonium hydroxide (J.T. Baker, 28–30%) and oleic acid (Fluka) were used as-received.

2.2. Synthesis

2.2.1. Synthesis of mPEG–PCL copolymer

mPEG–PCL diblock copolymers having 5000 g/mol mPEG and 5000 g/mol PCL were prepared through a ring-opening polymerization of ε-CL using an mPEG macroinitiator in the presence of stannous octoate catalyst. Dried mPEG (10.0 g, 0.002 mol), ε-CL (10.0 g, 0.228 mol) and stannous octoate (0.01 g, 1 mol%) were charged into a 100-ml two-neck round-bottom flask. The reaction proceeded at 120 °C for 48 h with magnetic stirring under N_2 atmosphere. The mixture was dissolved in $CHCl_3$ and precipitated in cold hexane. Copolymer purification process was repeated twice to remove unreacted species and it was then dried at 40 °C under reduced pressure.

2.2.2. Preparation of the copolymer-stabilized aqueous-based magnetite nanoparticles

The aqueous solutions of $FeCl_3$ (1.66 g in 20 ml deionized water) and $FeCl_2{\cdot}4H_2O$ (1.00 g in 20 ml deionized water) were mixed together with stirring. Black precipitant was observed once NH_4OH solution (25%, 20 ml) was added into the solution, indicating the formation of magnetite nanoparticles. The dispersion was continuously stirred for another 30 min to complete the reaction. The dispersion was centrifuged at 5000 rpm for 20 min and the aqueous supernatant was discarded. Oleic acid solution in hexane (2.5–10 wt% in 20 ml hexane) was then introduced into the magnetite dispersion with stirring. The dispersion was concentrated by evaporating hexane to obtain a black thick liquid of concentrated magnetite in hexane. To prepare the copolymer-stabilized nanoparticles, 20 ml of the dispersion in hexane was introduced into 20 ml of aqueous copolymer solution (1 wt% of copolymers). The mixtures were then ultrasonicated for 1–4 h to transfer the particles from hexane top layer to aqueous bottom layer. Hexane was evaporated by rigorous stirring at room temperature for another 30 min and the remaining dispersions were then centrifuged at 5000 rpm for 20 min to remove large aggregate. The copolymer–magnetite complex in water was then dialyzed against deionized water and refreshed twice at 24 h interval to remove excess copolymers from the dispersions. Precise concentrations of magnetite in the dispersions were determined by atomic absorption spectroscopy (AAS).

2.3. Characterization

2.3.1. Characterization of the mPEG–PCL copolymers

Proton NMR was performed on a 400 MHz Bruker NMR spectrometer using $CDCl_3$ as a solvent. FTIR was performed on a Perkin–Elmer Model 1600 Series FTIR Spectrophotometer. Neat samples were directly cast onto potassium chloride plates. Gel permeation chromatography (GPC) data were conducted on PLgel 10 μm mixed B2 columns and a refractive index detector. Tetrahydrofuran (THF) was used as a solvent with a flow rate of 1 ml/min at 30 °C.

2.3.2. Characterization of magnetite nanoparticles

Magnetite concentrations in dispersions were investigated by treating the samples with hot concentrated nitric acid followed by concentrated perchloric acid to obtain complete dissolution. Iron concentrations were analyzed by flame atomic absorption spectrometer (AAS) and calculated from sample responses relative to those of standards and blanks. Size of the particles and their size distribution were observed from transmission electron microscopy (TEM). TEM images were taken using a Philips Tecnai 12 operated at 120 kV equipped with Gatan model 782 CCD camera. The sample solution in water was cast onto carbon-coated copper grids and let to slowly evaporate at room temperature. Thermogravimetric analysis (TGA) was performed on SDTA 851 Mettler-Toledo at the temperature ranging between 25 and 600 °C at a heating rate of 20 °C/min under oxygen atmosphere. Magnetic properties of the polymer–magnetite complexes were measured in the solid state at room temperature using a Standard 7403 Series, Lakeshore vibrating sample magnetometer (VSM). The magnetic moment of each sample was investigated over a range of applied magnetic

fields from −10,000 to +10,000 G using 30 min sweep time. Mass specific magnetizations were calculated using the concentration of iron measured by atomic absorption spectrometer and assuming that all irons were in the form of magnetite. Indomethacin concentrations were determined using SPECORD S100 UV–vis spectrophotometer (Analytikjena AG) coupled with a photo diode array detector. A standard curve at $\lambda_{max} = 320$ nm UV absorbance [40,41] was established using identical conditions to calculate the amount of drug loaded on the particles.

2.3.3. Investigation of indomethacin entrapping efficiency of magnetite nanoparticles

Indomethacin was used as a model drug in the studies. To incorporate the drug to the particles, the drug solution (2 ml, 25 mg/ml in THF) was added dropwise with stirring to an aqueous dispersion of copolymer–magnetite complex (5 ml, 6.35% w/v of magnetite in water). The mixture was stirred for 30 min with heating to remove THF and to allow fully partitioning the drug into the hydrophobic shell surrounding the particles. The excess drug precipitated out form the mixture and was removed by centrifugation at 5000 rpm. Drug-loaded magnetite was then separated using an external magnet. Due to a good solubility of indomethacin in THF:ethanol solution (50:50%v/v), the solvent mixture was used to repeatedly extract the entrapped drug from the particles. After centrifugation to remove aggregated particles, the drug concentration in the supernatant was determined using UV–vis spectrophotometer. Entrapment efficiency and drug loading efficiency (DLE) were determined as follows:

$$\text{Entrapment efficiency (\%EE)} = \frac{\text{Weight of drug in nanoparticles}}{\text{Weight of loaded drug}} \times 100$$

$$\text{Drug loading efficiency (\%DLE)} = \frac{\text{Weight of drug in nanoparticles}}{\text{Weight of nanoparticles}} \times 100$$

Three different experiments were performed to obtain an average percent of each value.

3. Results and discussion

The aim of this research was to synthesize water dispersible magnetite nanoparticles containing hydrophobic inner shells for efficient entrapment of indomethacin-loaded drug and hydrophilic outer shells for a good dispersion in aqueous fluids. Amphiphilic block copolymers of mPEG–PCL in conjunction with oleic acid were used as steric stabilizers for this purpose. Hydrophobic PCL blocks can adsorb onto the pre-synthesized magnetite nanoparticles coated with oleic acid stabilizer, and hydrophilic mPEG blocks can protrude outward from the particle surface to provide steric stabilization. In addition, PCL blocks render the inner shells of the particles essentially degradable through hydrolysis reaction of ester linkages. This allows possible tuning of the molecular weight of hydrolyzable PCL blocks to control its degradation rate and in turn releasing rate of any entrapped hydrophobic drug from the particles.

The copolymers having the molecular weights of 5000 g/mol mPEG and 5000 g/mol PCL blocks were synthesized *via* a ring-opening polymerization of ε-CL monomers using mPEG as macroinitiators and stannous octoate as a catalyst. Single hydroxyl groups at the mPEG chain terminal allowed the copolymers to have mPEG–PCL diblock architecture. The molecular weight of PCL block was controlled by using 1 mol of mPEG for every mole of the copolymers. ^{1}H NMR was used to verify chain propagation of mPEG macroinitiator by observing the presence of methylene protons at the linkage between mPEG and PCL blocks (peak *c* at 4.20 ppm) (Fig. 2A). In addition, the shift of the signals of methylene protons in PCL repeating units (peaks *d*, *e*, *f*, *g* and *h* at 2.30, 1.64, 1.40, 1.64 and 4.06 ppm, respectively) compared to those of cyclic ε-CL monomers (2.25, 1.68, 1.26, 1.57 and 4.08 ppm, respectively) due to the release of ring strain also indicated the formation of PCL blocks. Molecular weights of PCL blocks were estimated from peak *d* (2.30 ppm) corresponding to the methylene protons adjacent to carbonyl groups in PCL repeating units in conjunction with methylene proton signals in the repeating units of mPEG (peak *b* at 3.64 ppm). It was found that the molecular weight of PCL block was 4900 g/mol, which was comparable to the targeted molecular weight (5000 g/mol PCL). In good agreement with ^{1}H NMR, the signal at 1724 cm^{-1} in the FTIR spectrum corresponding to the carbonyl group of ester linkages in PCL block also confirmed the ring-opening reaction (Fig. 2B). The signal at 3440 cm^{-1} indicated the remaining of hydroxyl groups at the chain ends of the copolymer. GPC revealed that the number average molecular weight ($\overline{M}_n$) of the copolymer was 12,000 g/mol with polydispersity index (PDI) about 1.52, which is broader than the corresponding mPEG homopolymer (PDI = 1.09, $\overline{M}_n$ = 5200 g/mol).

After coprecipitation of the iron precursors, the nanoparticles were stabilized with oleic acid and dispersed in hexane. The stabilizing mechanism of these particles arose from the chemi-sorption of carboxylate groups of oleic acid with magnetite nanoparticle surface and allowed C_{18} hydrocarbon to provide steric stabilization [39]. The concentration of the oleic acid-coated magnetite nanoparticles in hexane after removing large aggregate was approximately 8.6% wt/v. To transfer these nanoparticles to water phase, a copolymer aqueous solution with a certain concentration was introduced into the as-prepared magnetite dispersion in hexane. The hexane–water mixture was phase separated initially (Fig. 3).

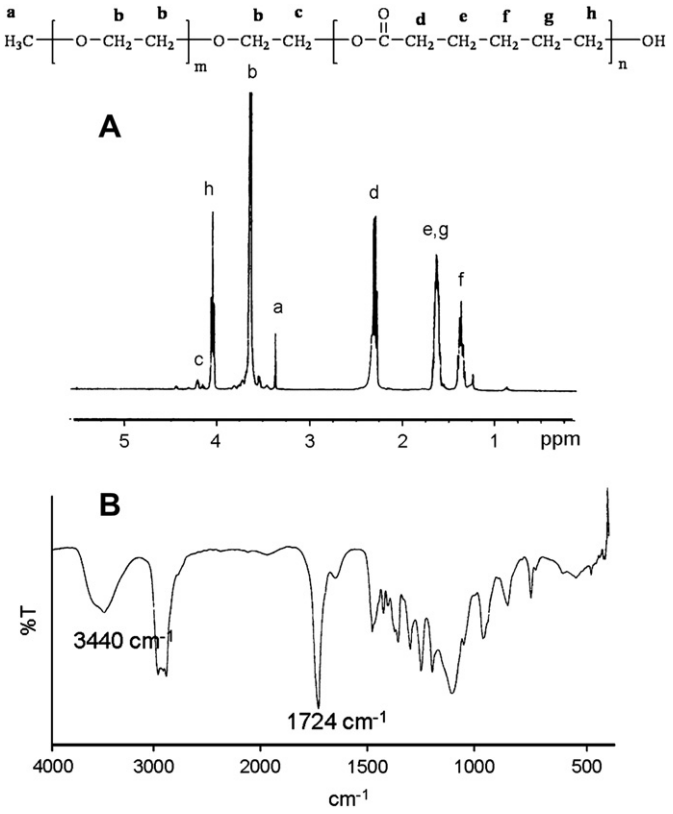

Fig. 2. (A) ^{1}H NMR and (B) FTIR spectra of the mPEG–PCL amphiphilic block copolymer.

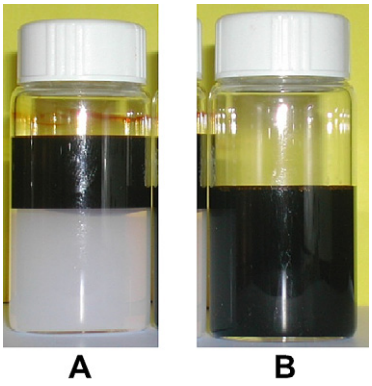

Fig. 3. Dispersions of (A) oleic acid-coated Fe_3O_4 nanoparticles dispersed in hexane (top layer) and the copolymer solution in water (bottom layer) and (B) oleic acid/copolymer-coated Fe_3O_4 nanoparticles in water after sonication and decanting hexane top layer.

After sonicating the mixture for approximately 1 h, water layer on the bottom of the mixture turned black indicating migration of the nanoparticles from hexane phase to water phase. It is hypothesized that due to amphiphilic nature of mPEG–PCL copolymers, hydrophobic PCL blocks aggregated in water and formed micellar core, while hydrophilic mPEG blocks dispersed in water and formed micellar corona. Once the hexane–water mixture was sonicated, the particles transferred from hexane phase to aqueous phase and were trapped into the micellar core due to physi-sorption interaction between oleic acid and hydrophobic PCL block. The particles were thus dispersible in water owing to mPEG block extended from the particle surface and prevented close proximity to their neighboring particles. An excess of oleic acid and the particles without copolymer coating dispersed in hexane top layer were then decanted.

The role of the copolymer on promoting dispersibility of the particles in water was investigated by observing FTIR spectra of the copolymer–magnetite complex dispersed in water and the aggregate. The copolymer–magnetite complex was dialyzed to remove an excess of the copolymer and freeze-dried to obtain FTIR samples in a solid form. Fig. 4A illustrates an FTIR spectrum of mPEG–PCL copolymer in comparison with that of the copolymer–magnetite complex (1.0 wt% copolymer concentration) (Fig. 4B). Carbonyl stretching of ester linkages (–OC=O, 1733 cm^{-1}) in conjunction with hydroxyl stretching (–OH, 3343 cm^{-1}) of hydroxyl-terminated PCL indicates the presence of PCL partitioning to the particle surface. In addition, the signal at 590 cm^{-1} in spectrum B corresponding to Fe–O bonds of the copolymer–magnetite complex was also observed [42].

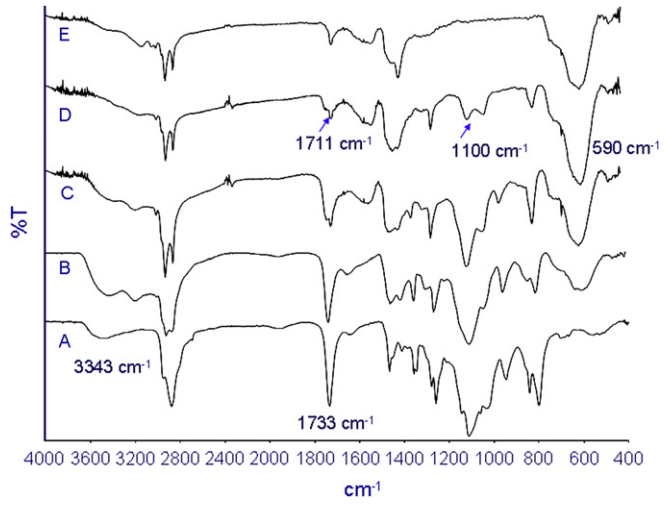

Fig. 4. FTIR spectra of (A) mPEG–PCL copolymer without magnetite, (B) copolymer–magnetite complex having 1 wt% of copolymer, (C) copolymer–magnetite complex having 0.5 wt% of copolymer, (D) aggregate from water phase, and (E) oleic acid–magnetite complex.

The intensity of FTIR signals of the complex was dependent on the copolymer concentration on the particle surface. Fig. 4B and C exhibits FTIR spectra of the copolymer–magnetite complexes having 1.0 and 0.5 wt% copolymer concentrations, respectively. It was observed that when the copolymer concentration in the complex was increased, the signals belonging to the copolymer, e.g. carbonyl and the finger print regions (1500–700 cm^{-1}), exhibited a gradual change toward those of the copolymer (Fig. 4A), indicating that more copolymer was bound to the particle surface. Spectrum D belongs to the aggregate from the dispersions obtained after centrifugation (Fig. 4D). This aggregate probably arose from an inadequate amount of the copolymer needed to stabilize the particles in water. In good agreement with this assumption, the weak signal at 1100 cm^{-1} corresponding to C–O–C stretching of mPEG indicates low amounts of the copolymer attached to the particle surface (Fig. 4D). Except for the 1100 cm^{-1} signal, this FTIR pattern is similar to that of the oleic acid–magnetite complex before coating with mPEG–PCL copolymers (Fig. 4E). In addition, the signal of Fe–O linkages in Fig. 4D was larger than those in (B) and (C) due to the higher content of Fe_3O_4 in the oleic acid–magnetite complex compared to the copolymer–magnetite complex.

The amounts of aggregate were strongly dependent on the copolymer concentrations in aqueous solutions. Fig. 5 exhibits the aqueous dispersions after dialysis and centrifugation to precipitate any large aggregate. As the copolymer concentrations were increased up to 1 wt%, there was no aggregate observed (Fig. 5b). It should be noted that the mass ratio of the copolymer to the oleic acid–coated magnetite at this concentration was about 1:9. Higher amount of aggregate accumulated at the bottom as lower concentration of the copolymer was used. When too low concentration of the copolymers was applied, the aqueous phase was transparent indicating that Fe_3O_4 nanoparticles barely dispersed in aqueous phase (Fig. 5f). Magnetite concentrations in aqueous dispersions a–f were 1.60, 1.45, 0.95, 0.75, 0.43 and 0% wt/v, respectively. This can be surmised that copolymer concentrations played an important role on dispersibility of the copolymer–magnetite complex in water.

Particle size and size distribution of magnetite nanoparticles were also investigated using transmission electron microscopy (TEM). A representative TEM image and size distribution of copolymer–magnetite complex dispersed in water having 1.0 wt% copolymer concentrations are illustrated in Fig. 6. Particle size was

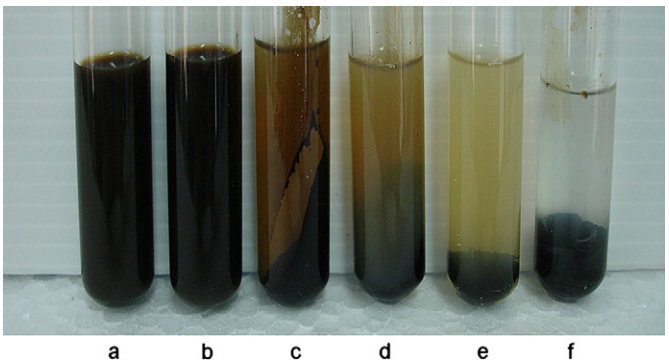

Fig. 5. Fe_3O_4 nanoparticle dispersions in water at (a) 5, (b) 1, (c) 0.5, (d) 0.1, (e) 0.01 and (f) 0.001 wt% of the copolymer concentrations.

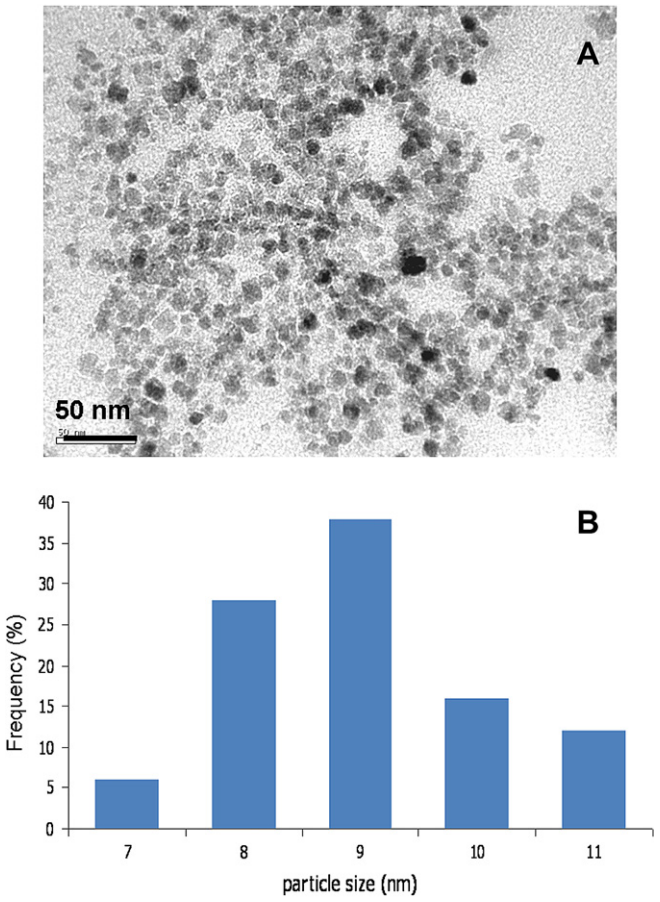

Fig. 6. (A) A TEM bright field image of copolymer–magnetite complex in water, and (B) particle size distribution with average particle size 9.0 ± 1.1 nm in diameter.

determined by measuring diameter of 100 particles in different regions of a given TEM grid. The particle size ranged between 7 and 11 nm in diameter with the average of approximately 9.0 ± 1.1 nm. The particle size of the dispersions having different copolymer concentrations was comparable to that in Fig. 6, indicating that the particle size was not dependent on the copolymer concentrations in the solutions.

In addition to the copolymer concentration, the concentration of oleic acid used to stabilize magnetite nanoparticles in hexane also played an important role on migration of the particles from hexane to aqueous phase. Table 1 shows the effect of oleic acid concentrations used as the primary surfactant on percent of magnetite in the complex and their magnetic properties. Percent of magnetite in copolymer–magnetite complex increased from 52 to 71% when the concentration of oleic acid used to form first-layer coating increased from 2.5% to 7.5% (dispersions A–C). An adequate amount of oleic acid might be necessary to obtain a well-defined first-layer hydrophobic coating before physisorption with PLC blocks of the copolymer and then transferring to water phase. However, further increase of the oleic acid concentration to 10% (dispersion D) did not further increase the percent of magnetite in the complex. Saturation magnetization (M_s) of these four dispersions ranged between 17 and 25 emu/g sample and the numbers tended to increase when the percent of magnetite in the complex increased. Interestingly, when taking percent of magnetite in the complex into account, M_s in emu/g magnetite unit of these four dispersions were close to each other. Similar experimental setup was used to study the influence of the copolymer on the magnetic properties of the core nanoparticles by fixing oleic acid concentration at 10% and varying the copolymer concentrations in the mixture. It was found that as the copolymer concentration was increased (0.01, 0.1, 0.5 and 1%), M_s in emu/g magnetite unit of these dispersions was comparable to each other (31–34 emu/g Fe_3O_4). The only difference observed between these dispersions was their dispersibility in aqueous media as shown in Fig. 5. These results indicated that magnetic properties of the core nanoparticles were not depended on either the concentrations of oleic acid primary surfactant or the copolymer secondary surfactant. It should be stated that M_s of oleic acid-coated magnetite (without copolymer coating) was about 34 emu/g Fe_3O_4. Thus, incorporation of the copolymers to the complex did not deteriorate magnetic properties of the nanoparticle core.

Time periods of ultrasonicating the water/hexane mixture of magnetite and copolymer also played a key role on magnetic properties of the particles. Table 2 shows the percent of magnetite in the copolymer–magnetite complex and M_s of the complex after ultrasonication for 1–4 h. Percent of magnetite in the complex ranged between 66 and 71% and did not significantly increased when time periods of ultrasonication were extended. However, the complex having only 1 h sonication possessed significantly low magnetic response as indicated by a low M_s value (dispersion E). This result suggested that magnetic properties of the particles were influenced by ultrasonicating time periods and at least 2 h of ultrasonication was required to obtain particles with good magnetic response. It is hypothesized that relatively small particles migrated to aqueous phase when only 1 h sonication was applied as indicated by the average particle size of 7.8 nm obtained from TEM analysis. Size of nanoparticles definitely influences their magnetic properties. Extension of ultrasonication time might further enhance phase-migration efficiency of the particles resulting in migration of large particles (9.0 nm) to aqueous phase and thus particles with high M_s values obtained. Representative hysteresis curves of dispersions A and E are illustrated in Fig. 7. It should be noted that dispersions A–H shown in Tables 1 and 2 have

Table 1
Effect of oleic acid concentrations on percent of magnetite in the complex and its magnetic properties

Dispersion	Conc. of oleic acid[a] (% wt/v)	% Fe_3O_4 in copolymer–magnetite complex[b]	M_s[c] (emu/g sample)	M_s[c] (emu/g Fe_3O_4)
A	2.5	52	17	32
B	5	59	19	32
C	7.5	71	25	35
D	10	71	23	33

[a] Concentrations of oleic acid used to disperse Fe_3O_4 in 20 ml hexane.
[b] Determined from aqueous layer of the mixture of 20 ml of 1 wt% of the copolymer and 20 ml hexane having different oleic acid concentrations and after 4 h sonication. %Fe_3O_4 in copolymer–magnetite complex determined from AAS.
[c] Calculated from the magnetic moment of the sample at 10,000 G.

Table 2
Effect of ultrasonicating time treatment on percent of magnetite in the complex and its magnetic properties

Dispersion	Time of ultrasonication[a] (h)	% Fe_3O_4 in copolymer–magnetite complex[b]	M_s[c] (emu/g sample)	M_s[c] (emu/g Fe_3O_4)
E	1	66	14	21
F	2	68	22	32
G	3	66	22	33
H	4	71	23	32

[a] Time period used to ultrasonicate the mixture of 20 ml of 1 wt% of the copolymer and 20 ml hexane having 10 wt% oleic acid.
[b] Determined from aqueous layer of the water/hexane mixture. %Fe_3O_4 in copolymer–magnetite complex determined from AAS.
[c] Calculated from the magnetic moment of the sample at 10,000 G.

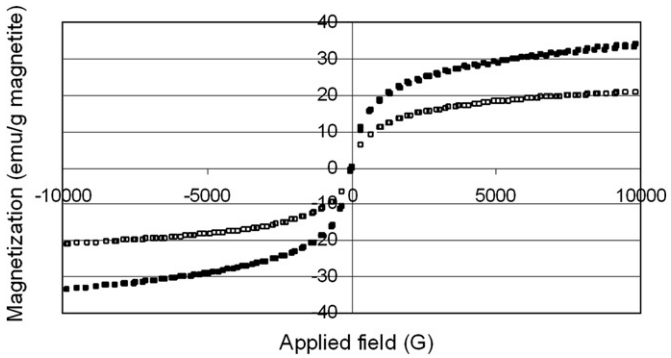

Fig. 7. Representative hysteresis curves of Fe_3O_4 nanoparticles of dispersion A (■) and E (□).

superparamagnetic properties at room temperature as indicated by the absence of reminance and coercivity upon removing an external applied magnetic field.

TGA was carried out to determine percent weight loss of the complexes, which manifested the amount of oleic acid and copolymer adsorbed on the particle surface (Fig. 8). The difference of the weight remaining at 600 °C between bare magnetite (90%) (Fig. 8A) and oleic acid-coated magnetite (31%) (Fig. 8B) was hypothetically the weight of oleic acid adsorbed on the nanoparticle surface. Similarly, the difference of the weight remaining between oleic acid-coated magnetite (31%) (Fig. 8B) and copolymer–magnetite complex (19%) (C) was the weight of the copolymer adsorbed on their surface. It was found that there was 59% oleic acid and only 12% of copolymer was adsorbed on the complex. Although only small amount of copolymer observed on their surface, the nanoparticles were well dispersed in water and remained stable at room temperature for more than a month without noticeable aggregation.

The studies on drug entrapping efficiency were accomplished to confirm the formation of bilayer surfactants with a hydrophobic inner layer. Indomethacin was selected as a model drug in the current studies due to its poor solubility in water. Therefore, it was hypothesized that the hydrophobic drug would partially precipitate in the inner hydrophobic shell of an oleic acid–PCL layer on the particle surface upon addition to the copolymer–magnetite complex. Percent entrapment efficiency (%EE) of the complex was approximately 43.2% (21.5 mg indomethacin entrapped/50 mg indomethacin loaded) and drug loading efficiency (%DLE) was $6.8 \pm 0.5\%$ wt/wt (68 μg/mg Fe_3O_4). This indicated that the copolymer-magnetite complex was effectively loaded with indomethacin and hypothetically any other hydrophobic drug should be also loaded in the formulation. The effect of the polymer block lengths and concentrations on drug-entrapped efficiency and drug releasing behavior are warranted for further investigation.

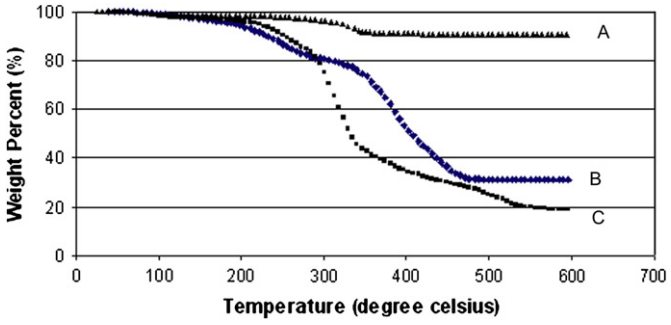

Fig. 8. TGA of (a) bare magnetite (▲), (b) oleic acid-coated magnetite (◆) and (c) copolymer–magnetite complex (■).

4. Conclusions

We reported a study on water dispersible magnetite nanoparticles stabilized with oleic acid primary surfactants and mPEG–PCL block copolymer secondary surfactants to form bilayer stabilizers having hydrophobic inner shell and hydrophilic corona. PCL was hypothesized to adsorb onto the particle surface coated with oleic acid and mPEG hydrophilic blocks extended to the carrier fluid to provide steric stabilization. Concentrations of both oleic acid and the copolymer influenced the percent of magnetite in the copolymer–magnetite complex dispersed in water. The particles were about 9.0 nm in diameter and exhibited superparamagnetic behavior at room temperature with M_s ranging between 21 and 35 emu/g magnetite. This copolymer–magnetite complex can be effectively loaded with indomethacin (%DLE = 68 μg/mg Fe_3O_4) with 42% EE. This complex was theoretically possible to load any other hydrophobic drug by partitioning to the hydrophobic shell on the particle surface. Tuning the molecular weights of mPEG and PLC blocks is warranted for further studies to investigate the influence of hydrophilic block lengths on particle stability in water and the effect of PCL block lengths, the hydrolysable moiety, on releasing rate of the drug from the particle.

Acknowledgement

The authors acknowledge The Thailand Research Fund (TRF) and Commission on Higher Education (CHE) (RMU4980006) for financial funding. SM thanks Center for Innovation in Chemistry: Postgraduate Education and Research Program in Chemistry (PERCH) for financial support. The authors also thank Dr. Umporn Weangmul for assistance in TEM technique and Assoc. Prof. Dr. Sakchai Witaya-areekul from the department of Pharmaceutical Science, Naresuan University, for his suggestion regarding the drug entrapping studies.

Appendix. Supplementary data

Supplementary data associated with this article can be found in the online version, at doi:10.1016/j.polymer.2008.07.003.

References

[1] Shen L, Stachowiak A, Fateen SEK, Laibinis PE, Hatton TA. Langmuir 2001;17:288.
[2] Pankhurst QA, Connolly J, Jones SK, Dobson JJ, Phys D. J Appl Phys 2003;36:167.
[3] Tartaj P, Morales MP, Veintemillas-Verdaguer S, Gonzalez-Carreno T, Serna CJ, Phys D. J Appl Phys 2003;36:182.
[4] Kim DK, Mikhaylova M, Wang FH, Keht J, Bjelke B, Zhang Y, et al. Chem Mater 2003;15:4343.
[5] Gamarra LF, Brito GES, Pontuschka WM, Amaro E, Parma AHC, Goya GF. J Magn Magn Mater 2005;289:439.
[6] Jun YW, Huh YM, Choi JS, Lee JH, Song HT, Kim S, et al. J Am Chem Soc 2005;127:573233.
[7] Cheng FY, Shieh DB, Yeh CS. Biomaterials 2005;26:729.
[8] Lawaczeck R, Menzel M, Pietsch H. Appl Organomet Chem 2004;18:506.
[9] Asmatulu R, Zalich MA, Claus RO, Riffle JS. J Magn Magn Mater 2005;292:108.
[10] Tan ST, Wendorff JH, Pietzonka C, Jia ZH, Wang GQ. Chem Phys Chem 2005;6:1461.
[11] Roger J, Pons JN, Massart R, Halbreich A, Bacri JC. Eur Phys J Appl Phys 1999;5:321.
[12] Liberti PA, Rao CG, Terstappen LWMM. J Magn Magn Mater 2001;225:301.
[13] Denizot B, Tanguy G, Hindre F, Rump E, Le Jeune JJ, Jallet P. J Colloid Interface Sci 1999;209:66.
[14] Yuan JJ, Armes SP, Takabayashi Y, Prassides K, Leite CAP, Galembeck F, et al. Langmuir 2006;22:10989.
[15] Guardia P, Batlle-Brugal B, Roca AG, Iglesias O, Morales MP, Serna CJ, et al. J Magn Magn Mater 2007;316:756.
[16] Si S, Li CL, Wang X, Yu D, Peng Q, Li Y. Cryst Growth Des 2005;5(2):391.
[17] Avdeev MV, Bica D, Vekas L, Marinica O, Balasoiu M, Aksenov VL, et al. J Magn Magn Mater 2007;311:6.
[18] Xianqiao L, Kaminski MD, Guan Y, Chen H, Liu H, Rosengart AJ. J Magn Magn Mater 2006;306:248.
[19] Wooding A, Kilner M, Lambrick DB. J Colloid Interface Sci 1991;144:236.

[20] Sahoo Y, Goodarzi A, Swihart MT, Ohulchanskyy TY, Kaur N, Furlani EP, et al. J Phys Chem B 2005;109:3879.
[21] Zhang Y, Zhang J. J Colloid Interface Sci 2005;283:352.
[22] Li Z, Chen H, Bao H, Gao M. Chem Mater 2004;16:1391.
[23] Xuan S, Hao L, Jiang W, Gong X, Hu Y, Chen Z. J Magn Magn Mater 2007;308:210.
[24] Zhang Y, Kohler N, Zhang M. Biomaterials 2002;23:1553.
[25] Zhao A, Yao P, Kang C, Yuan X, Chang J, Pu P. J Magn Magn Mater 2005;295:37.
[26] Zhang Y, Sun C, Kohler N, Zhang M. Biomed Microdevices 2004;6(1):33.
[27] Kohler N, Sun C, Wang J, Zhang M. Langmuir 2005;21:8858.
[28] Sonvico F, Mornet S, Vasseur S, Dubernet C, Jaillard D, Degrouard J, et al. Bioconjugate Chem 2005;16:1181.
[29] Kohler N, Fryxell GE, Zhang M. J Am Chem Soc 2004;126:7206.
[30] Mohapatra S, Mallick SK, Maiti TK, Ghosh SK, Pramanik P. Nanotechnology 2007;18:385102.
[31] Zhang J, Rana S, Srivastava RS, Misra RDK. Acta Biomater 2008;8:440.
[32] Lellouche JP, Senthil G, Joseph A, Buzhansky L, Bruce I, Bauminger ER, et al. J Am Chem Soc 2005;127:11998.
[33] Grancharov SG, Zeng H, Sun S, Wang SX, Brien SO, Murray CB, et al. Phys Chem B 2005;109:13030.
[34] Kim DK, Mikhaylova M, Zhang Y, Muhammed M. Chem Mater 2003;15:1617.
[35] Gomez-Lopera SA, Arias JL, Gallardo V, Delgado AV. Langmuir 2006;22:2816.
[36] Sun S, Zeng H, Robinson DB, Raoux S, Rice PM, Wang SX, et al. J Am Chem Soc 2004;126:273.
[37] Jain TK, Morales MA, Sahoo SK, Leslie-Pelecky DL, Labhasetwar V. Mol Pharm 2005;2(3):194.
[38] Zhang Q, Thomson MS, Carmichael-Baranauskas AY, Caba BL, Zalich MA, Lin YN, et al. Langmuir 2007;23:6927.
[39] Harris LA, Goff JD, Carmichael AY, Riffle JS, Harburn JJ, St. Pierre TG, et al. Chem Mater 2003;15:1367.
[40] Shin IG, Kim SY, Lee YM, Cho CS, Sung YK. J Controlled Release 1998;51:1.
[41] Kim SY, Shin IG, Lee YM. Biomaterials 1999;20:1033.
[42] Ke T, Honging D, Kang S. Chem Mater 2006;18:5273.